Itinerant ferromagnetism in rocksalt NdO epitaxial thin films

Daichi Saito,[1] Kenichi Kaminaga,[2] Daichi Oka,[1] and Tomoteru Fukumura[1,2,3,4]
[1]*Department of Chemistry, Graduate School of Science, Tohoku University, Sendai 980-8578, Japan*
[2]*WPI Advanced Institute for Materials Research and Core Research Cluster, Tohoku University, Sendai 980-8577, Japan*
[3]*Center for Science and Innovation in Spintronics, Organization for Advanced Studies, Tohoku University, Sendai 980-8577, Japan*
[4]*Center for Spintronics Research Network, Tohoku University, Sendai 980-8577, Japan*

(Received 16 November 2018; revised manuscript received 15 May 2019; published 13 June 2019)

Rocksalt NdO (001) epitaxial thin films were synthesized. Contrary to paramagnetic NdO bulk polycrystal in previous studies, NdO epitaxial thin films showed ferromagnetism with a Curie temperature of 19.1 ± 1.8 K, originating from dominant direct Nd−Nd exchange interaction owing to the small intercationic distance. In addition, negative magnetoresistance and an anomalous Hall effect were observed.

DOI: 10.1103/PhysRevMaterials.3.064407

I. INTRODUCTION

Lanthanoid compounds exhibit diverse electrical and magnetic properties owing to their $4f$ electrons interacting with itinerant electrons [1–3]. Among lanthanoid ions, stable neodymium trivalent ion shows strong magnetic anisotropy and orbital dominant magnetization because of partially filled $4f^3$ orbitals [4,5]. These features result in remarkable magnetic properties such as a maximum energy product of Nd-Fe-B magnets [6] and the anomalous Hall effect (AHE) in $Nd_2Mo_2O_7$ with geometrically frustrated pyrochlore structure [7]. Neodymium monochalcogenides and monopnictides, Nd*Ch*s except NdO (*Ch* = S, Se, Te) [8] and Nd*Pn*s (*Pn* = N, P, As, Sb) [9], have long been investigated because their simple rocksalt structure was suitable to model the magnetic interactions (Fig. 1). While Nd*Pn*s with Nd^{3+} ions are insulative to semimetallic electrical conduction depending on $p-f$ coupling strength [10–12], Nd*Ch*s exhibit metallic conduction because of $5d^1$ itinerant electrons in Nd^{2+} ion [8,13]. By contrast, magnetism in both Nd*X*s (*X* = *Ch*, *Pn*) is governed by intercationic distance between Nd ions, depending on anion size. In analogy with Eu*Ch*s [1], possible magnetic interactions among the Nd ions are ferromagnetic direct interaction, antiferromagnetic superexchange interaction, and long-range Ruderman-Kittel-Kasuya-Yosida (RKKY) interaction. The nearest-neighbor ferromagnetic exchange interaction increases with decreasing the intercationic distance, whereas the next-nearest-neighbor antiferromagnetic interaction is almost independent of the distance [1,14]. As a result, Nd*Pn*s are antiferromagnetic from NdSb to NdP through NdAs, with reduced Néel temperature with decreasing anionic size [9,15], and turns out to be ferromagnetic for NdN with rather high Curie temperature [12] (Fig. 1). Nd*Ch*s show a similar tendency from NdTe to NdS through NdSe [8,16] (Fig. 1). In NdS, noncollinear magnetic structure was observed, probably because of RKKY interaction mediated by the $5d^1$ itinerant electrons in Nd^{2+} ion [13,17]. Therefore, ferromagnetism is expected in NdO with a small lattice constant as a result of the competitive three exchange interactions. However, paramagnetism with metallic electrical conduction was reported in bulk NdO polycrystals nearly 40 years ago without subsequent studies [18,19]. This discrepancy could be most likely due to sample oxidization from the thermodynamically unstable NdO to very stable Nd_2O_3 in air [20]. In this study, we synthesized single-crystalline NdO epitaxial thin films and investigated their electrical and magnetic properties. The NdO epitaxial thin film was metallic as reported but showed ferromagnetism below the Curie temperature $T_C = 19.1 \pm 1.8$ K, being consistent with the chemical trend of Nd*X*s (Fig. 1).

II. EXPERIMENT

NdO epitaxial thin films were grown on $YAlO_3$ (110) substrates (pseudocubic $a = 5.22$ Å with lattice mismatch = −4.5%) at 250 °C with the pulsed laser deposition method under similar conditions as previous studies of rare-earth monoxides [21–23]. A Nd metal target was irradiated with a KrF excimer laser ($\lambda = 248$ nm) with oxygen pressures up to 3.0×10^{-8} Torr in an ultrahigh vacuum chamber. NdO thin films (typically 40 nm thick) were *in situ* capped with an ∼5-nm-thick amorphous AlO_x layer to prevent oxidation. Crystal structure and film orientation were analyzed by an x-ray diffractometer equipped with a four-axis diffractometer (Bruker AXS D8 Discover). The electrical resistivity ρ, carrier density, and mobility of Hall-bar patterned samples were measured by the four-probe and Hall effect measurements with a physical property measurement system (Quantum Design Model 6000). The magnetization measurements were performed by a superconducting quantum interference device magnetometer (Quantum Design, MPMS2) in which the diamagnetic signal of the $YAlO_3$ substrate and AlO_x layer was subtracted.

III. RESULTS AND DISCUSSION

From the x-ray diffraction $\theta - 2\theta$ pattern, only NdO 00*l* diffractions were observed without any secondary phase [Fig. 2(a)]. The FWHM of the rocking curve taken at the 002 peak maximum was 0.870°. The reciprocal space map represented the epitaxial relationship between the NdO film and $YAlO_3$ substrate as (001) NdO [110] // (110) $YAlO_3$ [001]. The lattice constants calculated from the two peaks

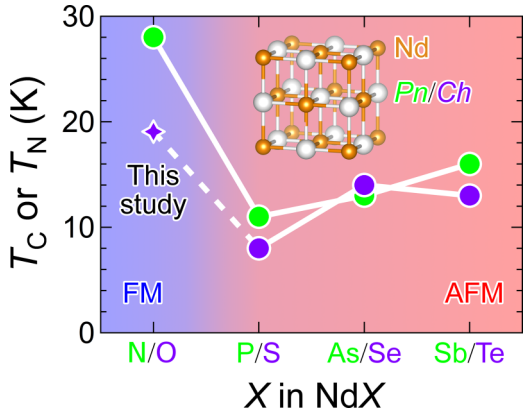

FIG. 1. Magnetic transition temperatures of Nd*Pn*s and Nd*Ch*s. Blue and red shaded areas correspond to ferromagnetic and antiferromagnetic phases, respectively. Inset shows the rocksalt structure of Nd*X*s.

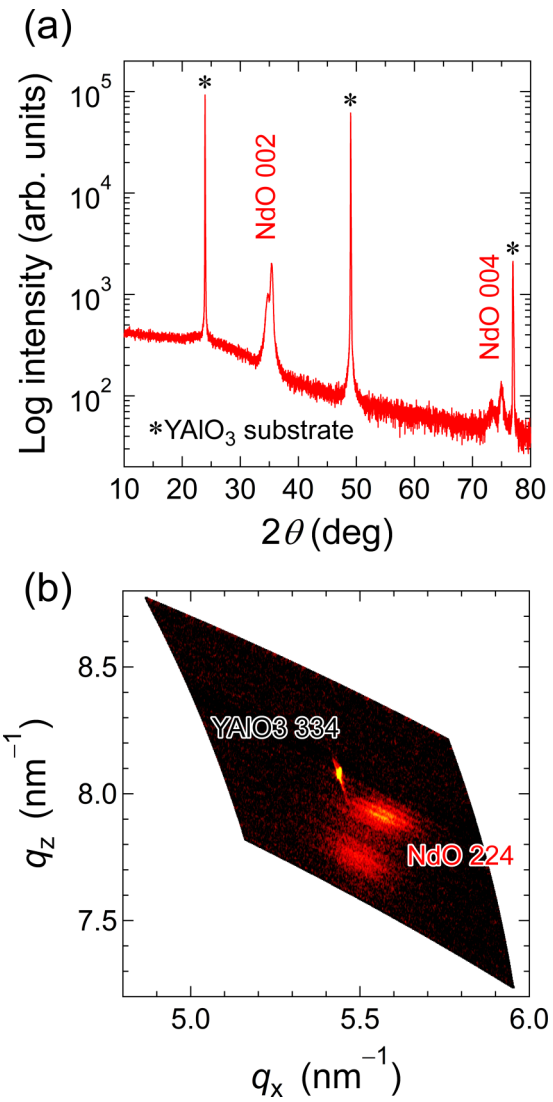

FIG. 2. (a) X-ray diffraction $\theta - 2\theta$ pattern and (b) reciprocal space map at around 224 diffraction for NdO (001) epitaxial thin film on $YAlO_3$ (110) substrate.

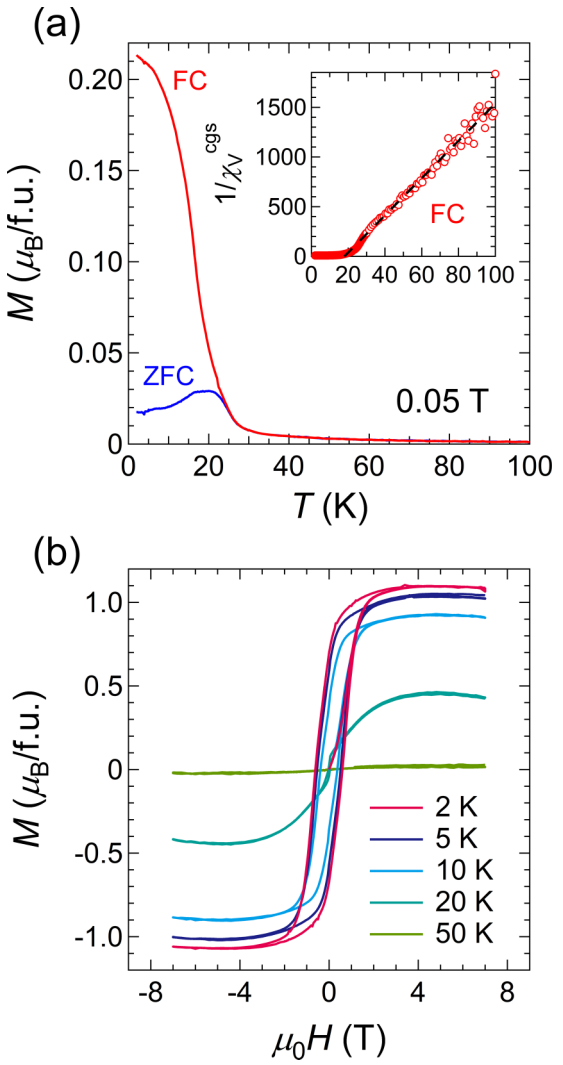

FIG. 3. (a) Temperature dependence of magnetization for NdO epitaxial thin film at 0.05 T (FC: red; ZFC: blue). Inset shows temperature dependence of inverse susceptibility. (b) Magnetic field dependence of magnetization at different temperatures from 2 to 100 K. Magnetic field was applied to the out-of-plane [001] direction in these measurements.

of the NdO epitaxial thin films, probably caused by different degrees of lattice strains, were $a = 5.08$ Å, $c = 5.05$ Å and $a = 5.14$ Å, $c = 5.16$ Å, respectively [Fig. 2(b)], being close to 4.994 ± 0.005 Å of bulk polycrystal [24]. Thinner films possessed a nonsplit 002 peak, but their influence on physical properties were not observed (see Supplemental Material [25]).

Figure 3(a) shows the temperature T dependence of magnetization for the NdO epitaxial thin film. The magnetization in field cooling (FC) significantly increased with decreasing temperature, deviating from that in zero field cooling (ZFC) below 25 K [26]. The Kouvel-Fischer plot indicated T_C of 19.1 ± 1.8 K (Fig. S4) [25]. Magnetic hysteresis was also observed below T_C in magnetization measurements [Fig. 3(b)]. The coercive field of 5000 Oe at 5 K was much higher than that of about 100 Oe for EuO (001) epitaxial thin films at 5 K [27,28], reflecting larger spin-orbit coupling of the $4f^3$ electron system

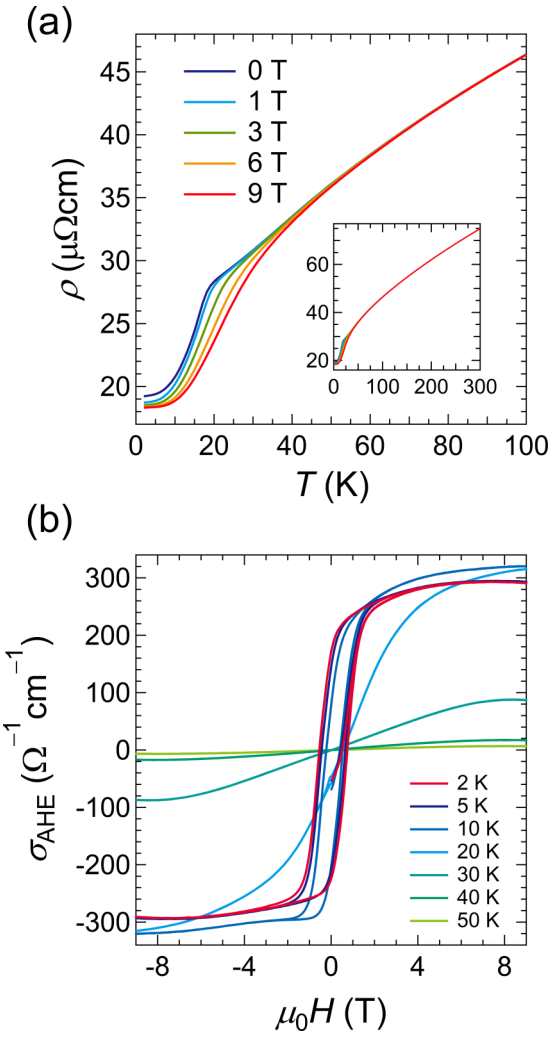

FIG. 4. (a) Temperature dependence of resistivity for NdO epitaxial thin film at various magnetic fields. Inset shows overall view of 2–300 K. (b) Magnetic field dependence of anomalous Hall conductivity at different temperatures from 2 to 50 K. The magnetic field was applied to the out-of-plane [001] direction.

in Nd ion compared to the $4f^7$ electron system in Eu ion [4,29]. Taking into account that only NdN is ferromagnetic among Nd*Pn*s, ferromagnetism in NdO suggests that direct ferromagnetic exchange interaction among Nd ions was dominant due to small oxide ions.

Magnetic parameters evaluated from the Curie-Weiss (CW) fitting above 30 K were the effective magnetic moment $m_{\rm eff} = 2.93\,\mu_{\rm B}$ and the Curie-Weiss temperature $\theta_{\rm CW} = 18$ K [inset of Fig. 3(a)]. The former was close to ideal $m_{\rm eff} = 3.62\,\mu_{\rm B}$ for a free Nd^{3+} ion with the tenfold degenerate $J = 9/2$ ($L = 6$, $S = 3/2$) ground state. On the other hand, the saturation magnetization observed in the magnetization curve was $1.1\mu_{\rm B}$ at 2 K, which is about 1/3 of the ideal $m_{\rm eff}$. Such a reduced magnetic moment was also reported for NdN thin film, attributed to crystal field splitting of the original ground state by symmetry lowering [12]. The ground-state multiplet of Nd ion in NdO is expected to split into a doublet Γ_6 and two quartets Γ_8 under octahedral crystal fields as in the case of NdN, NdS, and NdSe [13,30]. Such a splitting is likely negligible at high temperature due to thermal energy but could be discernible at low temperature, resulting in preferential population at the lower-lying state concomitant with reduced magnetic moment. Indeed, $m_{\rm eff}$ was strongly reduced to about 1 $\mu_{\rm B}$ under weak tetragonal lattice distortion of 0.2% in case of NdN thin film [12]. Considering a tetragonal distortion greater than 0.5% in the NdO epitaxial thin films, the small $m_{\rm eff}$ at low temperature could be attributed to such crystal field splitting.

T dependence of resistivity ρ showed a metallic ($d\rho/dT > 0$) behavior [Figs. 4(a) and 4(b)], as reported for bulk samples [18]. The carrier density and mobility at 300 K were 1.1×10^{23} cm^{-3} and 0.77 cm^2 V^{-1} s^{-1}, respectively. The measured carrier density was higher than the theoretical value of 3.02×10^{22} cm^{-3} under the assumption that each Nd ion provides one $5d^1$ itinerant electron, where the former could be possibly overestimated by the presence of paramagnetic AHE [31,32]. The resistivity showed nearly T-linear behavior for 20–300 K, followed by a sharp decrease below $T_{\rm C}$ similar to doped EuO [28], indicating significant $4f - 5d$ coupling in NdO. Since the anomalous Hall conductivity $\sigma_{\rm AHE}$ is a good measure of M [33], $\sigma_{\rm AHE}$ was calculated from the equation $\sigma_{\rm AHE} = \rho_{\rm AHE}/(\rho^2 + {\rho_{\rm AHE}}^2)$, where $\rho_{\rm AHE}$ is anomalous Hall resistivity. AHE below $T_{\rm C}$ showed clear hysteresis curves [Fig. 4(b)], similar to the magnetization curves [Fig. 3(b)]. The temperature dependence of the coercive field, defined as the half width of the hysteresis curve, for $\sigma_{\rm AHE}$ showed good coincidence with that for the magnetization, as shown in Fig. S5 of the Supplemental Material [25], indicating that ferromagnetism is the main origin for the AHE.

IV. SUMMARY

NdO epitaxial thin films were successfully synthesized. The temperature dependence of resistivity and magnetization indicated itinerant ferromagnetism of NdO below $T_{\rm C} = 19.1 \pm 1.8$ K, reflecting the dominant ferromagnetic direct exchange interaction as a result of the small oxygen ionic radius. Magnetization was significantly reduced from the ideal value, probably due to symmetry lowering similar to the case of NdN. The negative magnetoresistance and distinct AHE suggested the strong $4f - 5d$ coupling.

ACKNOWLEDGMENTS

We thank Yuji Matsumoto (Tohoku University) for help with the film thickness measurements. This work is supported by JSPS-KAKENHI (Grants No. 18H03872, No. 18K18935, and No. 26105002) and the Mitsubishi Foundation. Daichi Saito acknowledges support from GP-Spin at Tohoku University.

[1] T. Kasuya, J. Alloys Compd. **192**, 11 (1996).
[2] S. Gupta and K. G. Suresh, J. Alloys Compd. **618**, 562 (2015).
[3] S. V. Eliseeva and J.-C. G. Bünzli, New J. Chem. **35**, 1165 (2011).

[4] S. Chikazumi, *Physics of Ferromagnetism*, 2nd ed. (Oxford University Press, New York, 1997), Chap. 3, Sec. 2.
[5] G. Hrkac, T. G. Woodcock, C. Freeman, A. Goncharov, J. Dean, T. Schrefl, and O. Gutfleisch, Appl. Phys. Lett. **97**, 232511 (2010).
[6] J. Chaboy, L. M. García, F. Bartolomé, A. Marcelli, G. Cibin, H. Maruyama, S. Pizzini, A. Rogalev, J. B. Goedkoop, and J. Goulon, Phys. Rev. B **57**, 8424 (1998).
[7] Y. Taguchi, Y. Oohara, H. Yoshizawa, N. Nagaosa, and Y. Tokura, Science **291**, 2573 (2001).
[8] P. Schobinger-Papamantellos, A. Niggli, P. Fischer, E. Kaldis, and V. Hildebrandt, J. Phys. C **7**, 2023 (1974).
[9] P. Schobinger-Papamantellos, P. Fischer, O. Vogt, and E. Kaldis, J. Phys. C **6**, 725 (1973).
[10] M. De and S. K. De, J. Phys. Chem. Solids **60**, 337 (1999).
[11] N. Wakeham, E. D. Bauer, M. Neupane, and F. Ronning, Phys. Rev. B **93**, 205152 (2016).
[12] E.-M. Anton, J. F. McNulty, B. J. Ruck, M. Suzuki, M. Mizumaki, V. N. Antonov, J. W. Quilty, N. Strickland, and H. J. Trodahl, Phys. Rev. B **93**, 064431 (2016).
[13] A. Furrer and E. Warmining, J. Phys. C **7**, 3365 (1974).
[14] T. R. McGuire, B. E. Argyle, M. W. Shafer, and J. S. Smart, J. Appl. Phys. **34**, 1345 (1963).
[15] T. Tsuchida, Y. Nakamura, and T. Kaneko, J. Phys. Soc. Jpn. **26**, 284 (1969).
[16] G. A. Smolenskii, V. P. Zhuze, V. E. Adamyan, and G. M. Loginov, Phys. Status Solidi B **18**, 873 (1966).
[17] I. V. Golosovskii and V. P. Plakhty, Phys. Status Solidi B **56**, 61 (1973).
[18] J. M. Leger, P. Aimonino, J. Loriers, P. Dordor, and B. Coqblin, Phys. Lett. **80**, 325 (1980).
[19] G. Krill, M. F. Ravet, J. P. Kappler, L. Abadli, J. M. Leger, N. Yacoubi, and C. Loriers, Solid State Commun. **33**, 351 (1980).
[20] J. M. Leger, N. Yacoubi, and J. Loriers, J. Solid State Chem. **36**, 261 (1981).
[21] K. Kaminaga, R. Sei, K. Hayashi, N. Happo, H. Tajiri, D. Oka, T. Fukumura, and T. Hasegawa, Appl. Phys. Lett. **108**, 122102 (2016).
[22] Y. Uchida, K. Kaminaga, T. Fukumura, and T. Hasegawa, Phys. Rev. B **95**, 125111 (2017).
[23] K. Kaminaga, D. Oka, T. Hasegawa, and T. Fukumura, J. Am. Chem. Soc. **140**, 6754 (2018).
[24] J. M. Leger, N. Yacoubi, and J. Loriers, Inorg. Chem. **19**, 2252 (1980).
[25] See Supplemental Material at http://link.aps.org/supplemental/10.1103/PhysRevMaterials.3.064407 for the magnetic and electrical measurements for thinner NdO epitaxial thin films, the Kouvel-Fischer plot, and temperature dependence of coercive field for thicker NdO films.
[26] A kink at 5 K in $M-T$ curve (FC) may be caused by an overestimation of background signal of the substrate and/or $4f-4f$ antiferromagnetic coupling.
[27] R. W. Ulbricht, A. Schmehl, T. Heeg, J. Schubert, and D. G. Schlom, Appl. Phys. Lett. **93**, 102105 (2008).
[28] T. Yamasaki, K. Ueno, A. Tsukazaki, T. Fukumura, and M. Kawasaki, Appl. Phys. Lett. **98**, 082116 (2011).
[29] A. Enders, R. Skomski, and D. J. Sellmyer, in *Nanoscale Magnetic Materials and Applications*, edited by J. P. Liu, E. Fullerton, O. Gutfleisch, and D. J. Sellmyer (Springer, New York, 2009), Chap. 3, Sec. 3.
[30] D. P. Schumacher and W. E. Wallace, Inorg. Chem. **5**, 1563 (1966).
[31] J. J. Rhyne, Phys. Rev. **172**, 523 (1968).
[32] F. Matsukura, H. Ohno, A. Shen, and Y. Sugawara, Phys. Rev. B **57**, R2037(R) (1998).
[33] N. Nagaosa, J. Sinova, S. Onoda, A. H. MacDonald, and N. P. Ong, Rev. Mod. Phys. **82**, 1539 (2010).